HHS Public Access

Author manuscript

J Mech Behav Biomed Mater. Author manuscript; available in PMC 2020 January 01.

Published in final edited form as:

J Mech Behav Biomed Mater. 2019 January ; 89: 9–12. doi:10.1016/j.jmbbm.2018.08.053.

Mechanical and Structural Analysis of the Pulmonary Valve in Congenital Heart Defects: A Presentation of Two Case Studies

Fatiesa Sulejmani[1], **Anastassia Pokutta-Paskaleva**[1], **Olga Salazar**[2], **Mohsen Karimi**[3], and **Wei Sun**[1,*]

[1]Tissue Mechanics Laboratory, The Wallace H. Coulter Department of Biomedical Engineering, Georgia Institute of Technology and Emory University, Atlanta, GA

[2]Pediatric Cardiology, Connecticut Children's Medical Center, Hartford, CT

[3]Pediatric Cardiac Surgery, Yale-New Haven Children's Hospital & Connecticut Children's Medical Center, Hartford, CT

Abstract

Objective: Congenital Heart Disease (CHD) is the leading cause of pediatric mortality, with many cases affecting the right ventricular outflow tract (RVOT) or pulmonary valve (PV). Understanding the mechanics of the disease condition can provide insight into development of durable repair techniques and bioengineered replacement devices. This work presents a mechanical and structural analysis of the pulmonary valve of two pediatric cases.

Methods: Two PV tissues were excised as part of the operative procedure. One PV was obtained from a 9-month- old with Noonan syndrome (Patient 1) and the other from a 6-month-old with tricuspid atresia (Patient 2). The leaflets were subjected to planar biaxial tensile testing and second harmonic generation (SHG) imaging for mechanical and structural evaluation.

Results and Discussion: Patient 1 exhibited a more anisotropic mechanical response than Patient 2, with sample stiffness on par with that of adult PV tissue. Additionally, both samples showed radial and circumferential alignment of collagen fibers on the ventricularis and fibrosa sides of the leaflets, respectively. Collagen fibers on the fibrosa side were also more crimped than on the ventricularis side.

Keywords

Pediatric; Pulmonary Valve; Congenital Heart Defect; CHD; Mechanics; Collagen; Atrial Septal Defect; Tricuspid Atresia

[*]For correspondence: Wei Sun, Ph.D., 206 Technology Enterprise Park, Georgia Institute of Technology, 387 Technology Circle, Atlanta, GA 30313-2412. Phone: (404) 385-1245. wei.sun@bme.gatech.edu.

Conflicts of Interest

None.

1. Introduction

Congenital Heart Defects (CHD) are the most common birth defect, affecting one out of every 100 live births in the United States and accounting for about 40,000 children per year [1–3]. CHD encompasses a wide range of cardiac anomalies, which invariably affects other organ systems [4]. CHD is typically grouped in the following categories [5]: cyanotic and acyanotic lesions, left-sided cardiac obstructive lesions, right sided cardiac obstructive lesions, and complex mixing lesions .

It is estimated that up to 20% of CHD children have specific heart defects that involve the right ventricular outflow tract (RVOT) and pulmonary valve (PV), over half of which consist of lesions associated with decreased pulmonary blood flow [3, 6]. PV stenosis and atresia (lack of valve formation), tricuspid valve atresia, Ebstein's anomaly, and the tetralogy of Fallot all fall under this category [1].

The etiology of CHD remains largely unknown [1, 4, 7]. As pediatric patients are typically subjected to multiple invasive procedures throughout their lifetimes in order to normalize pulmonary blood flow [8, 9], a better understanding of the disease state is necessary for the development of durable repair techniques and replacement devices, particularly as relates to tissue engineering and scaffold materials [10–12].

This undertaking has proven difficult in the past due to the limited availability of published data and the small size of the samples, which have led to substantial difficulties in mechanical testing. Despite these limitations, efforts have been devoted towards investigating the human pediatric aorta [13–15] and pulmonary artery [15–17], but no evaluation of valvular mechanics, to our knowledge, has been published.

To address these gaps in the literature, the following report presents the mechanical and structural behavior of PV leaflets from two pediatric cases with different disease etiologies. Properties were evaluated through planar biaxial tensile testing and second harmonic generation (SHG) imaging.

2. Materials and Methods

2.1. Patient Characteristics

Pulmonary leaflets from two pediatric patients with different valvar pathology were obtained from Connecticut Children's Medical Center (Hartford, CT), as shown in Figure 1. These tissue samples were obtained as part of the surgical procedure, which would have been otherwise discarded. The study was approved by the Georgia Institute of Technology Institutional Review Board. Sample thickness was measured and averaged in three distinct locations throughout the testing region using a Mitutoyo 7301 rotating thickness gage (Aurora, IL, ± 0.01 mm resolution).

Patient 1: 9-month-old male infant with diagnosis of Noonan syndrome, dysplastic pulmonary valve, supra-valvar pulmonary stenosis and atrial septal defect. The patient underwent two pulmonary balloon valvuloplasties.

Patient 2: 6-month-old female infant with tricuspid atresia, normally related great arteries, restrictive VSD and valvar pulmonary stenosis.

2.2. Biaxial Tensile Testing

Samples were subjected to biaxial tensile testing as per Sacks and Sun [18]. Briefly, a square section of the pulmonary valve was delimited by 8 suture hooks, 2 per side, such that the circumferential direction corresponded with the X_1 testing axis and the radial with the X_2. The sample was mounted onto a testing machine in a trampoline-like fashion, and submerged in a 0.9% saline solution maintained at 37° Celsius for the duration of the test. A stress-controlled testing protocol was administered, such that the ratio of the normal Lagrangian stress components P_{11}:P_{22} was predefined with shear terms $P_{12} = P_{21} = 0$. Samples were subjected to a minimum of 30 equibiaxial preconditioning cycles, followed by testing protocols with varied P_{11}:P_{22} ratio. Equibiaxial results are reported, with all biaxial plots showing Green Strain, defined as $E = ½ (F^TF – I)$, and Second Piola-Kirchoff Stress, S. Stiffness was evaluated by means of the upper tangent modulus (Figure 2).

2.3. Structural Imaging

Tissues were imaged on a Zeiss 710 NLO inverted confocal microscope (Carl Zeiss Microscopy, LLC, Thornwood, NY, USA) equipped with a mode-locked Ti:Sapphire Chameleon Ultra laser (Coherent Inc., Santa Clara, CA) in combination with non-descanned detection (NDD) to look at the collagen fibers. The laser was set to 800 nm and emission was filtered from 380–430 nm. Samples were kept hydrated with saline solution during imaging to prevent drying artifacts and SHG was collected from the fibrosa and ventricularis sides of the tissue on the belly of the leaflet using a Plan-Apochromat 40x oil immersion objective. Zeiss ZEN software was used to visualize and export image stacks for analysis.

3. Results and Discussion

As shown in Figures 3 and 4, the two samples presented markedly different mechanical and structural properties, despite being from patients of similar ages (9 and 6 months for Patients 1 and 2, respectively). Similar to healthy adult and animal PV leaflets [20, 21], anisotropy was seen in both pediatric samples, with the circumferential direction being stiffer than the radial direction. Additionally, Patient 2 exhibited a less extensible mechanical response along the radial direction (maximum strains of 0.4 vs. 0.2 for Patients 1 and 2, respectively), but was more extensible along the circumferential direction. Overall, Patient 2 exhibited a more isotropic response than Patient 1.

Previously published adult data from our lab shows PV stiffness at 5647 and 2179 kPa along the circumferential and radial directions, respectively [21]. It is interesting to note that the leaflet stiffness from the stenotic tissue of Patient 1 (10052 kPa and 3807 kPa in the post-transitional regions along the circumferential and radial directions respectively) was stiffer than that of adult cardiac tissue, while that of Patient 2 was more compliant along the circumferential direction (2779 kPa), but on par with that of much older adults in the radial direction (764 kPa). As tissue has been known to stiffen with age, the comparable stiffness

of these tissues between pediatric tissue and that of older adults points to the extent of the mechanical effects of their diseased states.

Structurally, the leaflets exhibited similar collagen structure on each side, with straighter collagen fibers on the ventricularis side compared to the more tightly crimped collagen structure of the fibrosa side for both patients. Moreover, the collagen fibers of the ventricularis side were predominantly aligned in the radial direction for both patients, while on the fibrosa side they were more aligned along the circumferential direction. These results are consistent with previously published human and animal studies investigating collagen fiber alignment [22–24]. Patient 1 showed a higher variation of collagen fiber orientation in the fibrosa side (average fiber orientation: 47.8 ± 18.1 ° and −14.4 ± 34.14° for the ventricularis and fibrosa sides, respectively), while Patient 2 had higher variations in the ventricularis side (average fiber orientation: 86.4 ± 38.1 ° and 2.6 ± 1° for the ventricularis and fibrosa sides, respectively). The less organized distribution of collagen fibers in Patient 2 suggests remodeling on the ventricularis side [25], a point of interest for future studies investigating cardiac remodeling as a result of tricuspid atresia.

4. Conclusions

This study investigated the mechanical and structural behavior of PV leaflets from two pediatric CHD cases through planar biaxial tensile testing and SHG imaging. The two leaflets showed relatively similar collagenous structure and distribution in the two leaflets, but differing in their mechanical responses. Patient 2, suffering from tricuspid atresia, had more isotropic leaflet behavior than Patient 1, who suffered from a dysplastic PV. Interestingly, tissue stiffness was comparable to or stiffer than that of adult human PV leaflets. Continued investigation of the mechanics and structure of CHD patients can lead to a deeper understanding of this complex mechanical and structural disease environment and to future development of advanced repair and replacement devices and techniques.

Acknowledgments

This study was funded in part by NIH HL104080 and HL127570 grants.

References

[1]. Hoffman JIE, Kaplan S. The incidence of congenital heart disease. Journal of the American College of Cardiology 2002;39:1890–900. [PubMed: 12084585]

[2]. Reller MD, Strickland MJ, Riehle-Colarusso T, Mahle WT, Correa A. Prevalence of Congenital Heart Defects in Metropolitan Atlanta, 1998–2005. The Journal of Pediatrics 2008;153:807–13. [PubMed: 18657826]

[3]. Hoffman JIE. Congenital Heart Disease: Incidence and Inheritance. Pediatric Clinics of North America 1990;37:25–43. [PubMed: 2408002]

[4]. Srivastava D Congenital heart defects: trapping the genetic culprits. Circulation research 2000;86:917–8. [PubMed: 10807859]

[5]. St. Louis JD Introduction to Congenital Heart Disease: Nomenclature and Classification. Cardiovascular Pediatric Critical Illness and Injury 2009:1–3.

[6]. Mai CT, Riehle-Colarusso T, O'Halloran A, Cragan JD, Olney RS, Lin A, et al. Selected birth defects data from population-based birth defects surveillance programs in the United States, 2005–2009: Featuring critical congenital heart defects targeted for pulse oximetry screening.

Birth Defects Research Part A: Clinical and Molecular Teratology 2012;94:970–83. [PubMed: 24083317]

[7]. Pierpont ME, Basson CT, Benson DW, Gelb BD, Giglia TM, Goldmuntz E, et al. Genetic basis for congenital heart defects: current knowledge. Circulation 2007;115:3015–38. [PubMed: 17519398]

[8]. Castaneda AR, Mayer JE, Jonas RA, Lock JE, Wessel DL, Hickey PR. The neonate with critical congenital heart disease: repair--a surgical challenge. J Thorac Cardiovasc Surg 1989;98:869–75. [PubMed: 2811420]

[9]. Morris CD, Menashe VD. 25-year mortality after surgical repair of congenital heart defect in childhood: A population-based cohort study. JAMA 1991;266:3447–52. [PubMed: 1744959]

[10]. Engelmayr GC, Hildebrand DK, Sutherland FWH, Mayer JE, Sacks MS. A novel bioreactor for the dynamic flexural stimulation of tissue engineered heart valve biomaterials. Biomaterials 2003;24:2523–32. [PubMed: 12695079]

[11]. Korossis SA, Booth C, Wilcox HE, Watterson KG, Kearney JN, Fisher J, et al. Tissue engineering of cardiac valve prostheses II: biomechanical characterization of decellularized porcine aortic heart valves. The Journal of heart valve disease 2002;11:463–71. [PubMed: 12150291]

[12]. Patterson JT, Gilliland T, Maxfield MW, Church S, Naito Y, Shinoka T, et al. Tissue-engineered vascular grafts for use in the treatment of congenital heart disease: from the bench to the clinic and back again. Regenerative medicine 2012;7:409–19. [PubMed: 22594331]

[13]. Ong CM, Canter CE, Gutierrez FR, Sekarski DR, Goldring DR. Increased stiffness and persistent narrowing of the aorta after successful repair of coarctation of the aorta: Relationship to left ventricular mass and blood pressure at rest and with exercise. American Heart Journal 1992;123:1594–600. [PubMed: 1595541]

[14]. Reed CM, Fox ME, Alpert BS. Aortic biomechanical properties in pediatric patients with the marfan syndrome, and the effects of atenolol. The American Journal of Cardiology 1993;71:606–8. [PubMed: 8438752]

[15]. Niwa K, Perloff JK, Bhuta SM, Laks H, Drinkwater DC, Child JS, et al. Structural abnormalities of great arterial walls in congenital heart disease. Circulation 2001;103:393–400. [PubMed: 11157691]

[16]. Cabrera MS, Oomens CWJ, Bouten CVC, Bogers AJJC, Hoerstrup SP, Baaijens FPT. Mechanical analysis of ovine and pediatric pulmonary artery for heart valve stent design. Journal of Biomechanics 2013;46:2075–81. [PubMed: 23849135]

[17]. Weinberg CE, Hertzberg JR, Shandas R. Use of intravascular ultrasound to measure local compliance of the pediatric pulmonary artery: In vitro studies. Journal of the American Society of Echocardiography 2002;15:1507–14. [PubMed: 12464920]

[18]. Sacks MS, Sun W. Multiaxial mechanical behavior of biological materials. Annual review of biomedical engineering 2003;5:251–84.

[19]. Pham T, Sulejmani F, Shin E, Wang D, Sun W. Quantification and comparison of mechanical properties of four human cardiac valves. Acta Biomater 2017 (in-review).

[20]. Billiar KL, Sacks MS. Biaxial mechanical properties of the natural and glutaraldehyde treated aortic valve cusp-Part I: Experimental results. Transactions-American Society of Mechanical Engineers Journal of Biomechanical Engineering 2000;122:23–30.

[21]. Pham T, Sulejmani F, Shin E, Wang D, Sun W. Quantification and comparison of the mechanical properties of four human cardiac valves. Acta Biomaterialia 2017;54:345–55. [PubMed: 28336153]

[22]. Tseng H, Grande-Allen KJ. Elastic fibers in the aortic valve spongiosa: a fresh perspective on its structure and role in overall tissue function. Acta biomaterialia 2011;7:2101–8. [PubMed: 21255691]

[23]. Stella JA, Sacks MS. On the biaxial mechanical properties of the layers of the aortic valve leaflet. Journal of biomechanical engineering 2007;129:757–66. [PubMed: 17887902]

[24]. Latif N, Sarathchandra P, Taylor PM, Antoniw J, Yacoub MH. Localization and pattern of expression of extracellular matrix components in human heart valves. The Journal of heart valve disease 2005;14:218–27. [PubMed: 15792183]

[25]. Phillippi JA, Green BR, Eskay MA, Kotlarczyk MP, Hill MR, Robertson AM, et al. Mechanism of aortic medial matrix remodeling is distinct in patients with bicuspid aortic valve. J Thorac Cardiovasc Surg 2014;147:1056–64. [PubMed: 23764410]

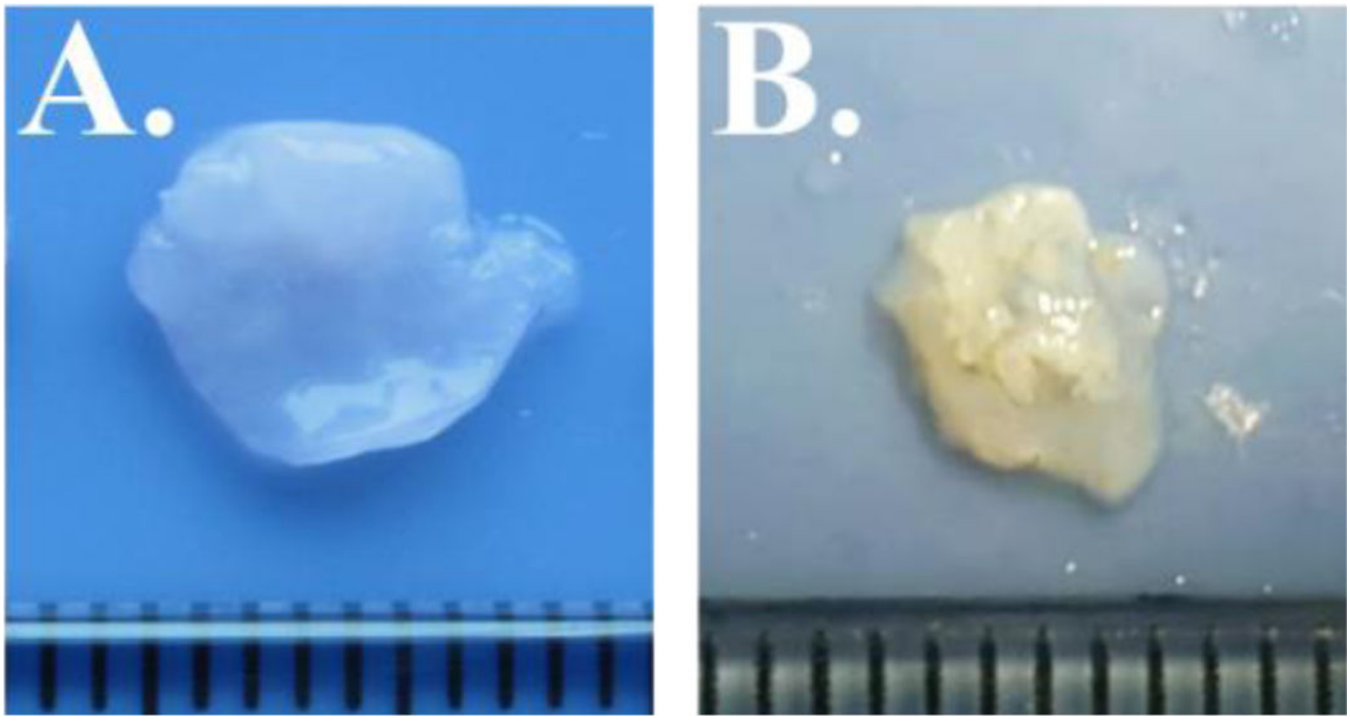

Figure 1.
PV leaflet samples for Patient 1 (A) and Patient 2 (B). Ruler tick marks indicate 1 mm.

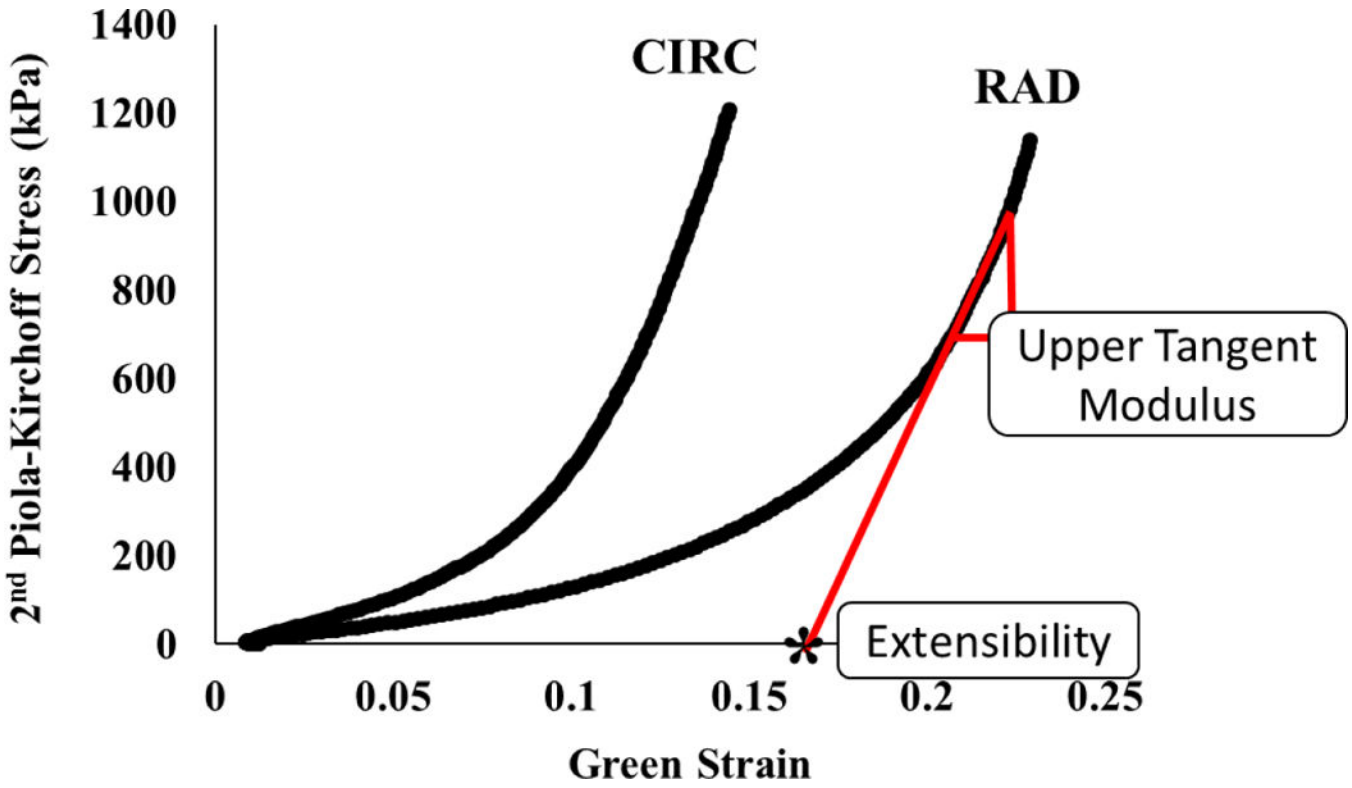

Figure 2.
Evaluation of stiffness and extensibility.

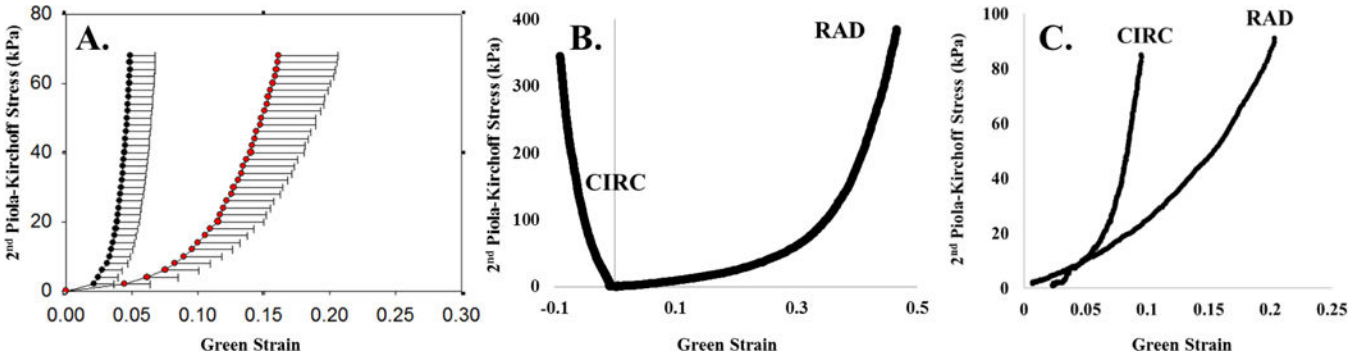

Figure 3.

Equibiaxial response curve for (A) aged human pulmonary leaflet, (B) Patient 1, (C) Patient 2. Panel A is adopted from Pham et al. [19].

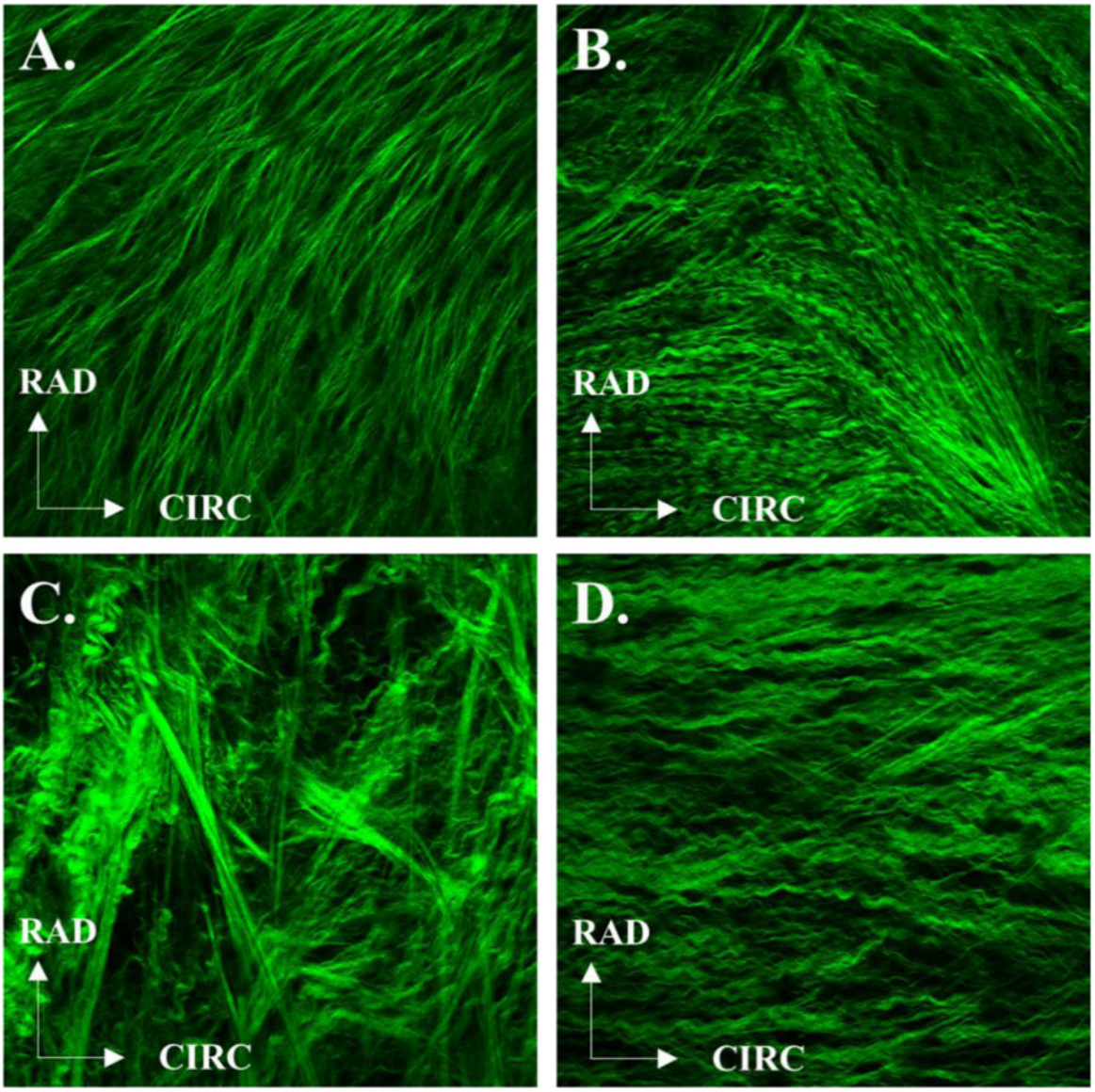

Figure 4.
Representative SHG images from the respective ventricularis and fibrosa sides of the PV leaflet for Patient 1 (A, B) and Patient 2 (C, D).